Formation of Mn-derived impurity band in III-Mn-V alloys by valence band anticrossing

K. Alberi,[1,2] K. M. Yu,[1] P. R. Stone,[1,2] O. D. Dubon,[1,2] W. Walukiewicz,[1,*] T. Wojtowicz,[3] X. Liu,[4] and J. K. Furdyna[4]

[1]*Materials Sciences Division, Lawrence Berkeley National Laboratory, Berkeley, California 94720, USA*

[2]*Department of Materials Science and Engineering, University of California, Berkeley, California 94720, USA*

[3]*Institute of Physics, Polish Academy of Sciences, 02-668 Warsaw, Poland*

[4]*Department of Physics, University of Notre Dame, Notre Dame, Indiana 46556, USA*

While the support for the existence of a Mn-derived impurity band in the diluted magnetic semiconductor $Ga_{1-x}Mn_xAs$ has recently increased, a detailed quantitative analysis of its formation and properties is still incomplete. Here, we show that such an impurity band arises as the result of an anticrossing interaction between the extended states of the GaAs valence band and the strongly localized Mn states according to the valence band anticrossing model. The anticrossing interpretation is substantiated by optical measurements that reveal a shift in the band gap of GaAs upon the addition of Mn and it also explains the remarkably low hole mobility in this alloy. Furthermore, the presence of a Mn-derived impurity band correctly accounts for the metal-to-insulator transition experimentally observed in $Ga_{1-x}Mn_xAs_{1-y}(N,P)_y$ with $y \leq 0.02$.

I. INTRODUCTION

Undoubtedly the most extensively investigated of the diluted magnetic semiconductors (DMSs) is $Ga_{1-x}Mn_xAs$, which has provided the foundation for the well-established description of ferromagnetism in semiconductors presented by the Zener model.[1] In fact, the anticipated magnetic and electrical properties of other III-Mn-pnictide DMSs are routinely extrapolated from those of $Ga_{1-x}Mn_xAs$ based on trends in the binding energy of the Mn acceptor level and the strength of the *p-d* exchange.[2] Despite the relative success of this approach, inconsistencies remain between the traditional picture of hole transport within this material, and that supported by recent theoretical and experimental investigations. Within the realm of the Zener model, Mn is initially expected to form an impurity band that eventually merges with the GaAs valence band at higher impurity densities ($x > 0.02$) according to the Mott theory for the metal-to-insulator transition (MIT).[1,3] However, several theoretical examinations based on both *ab initio* first-principles band-structure calculations and the dynamical mean-field theory (DMFT) approach, which assume a strong exchange coupling between the Mn and GaAs spin states, suggest the presence of a detached Mn-derived impurity band at all values of x.[4–6] A number of experimental investigations also support the impurity band picture. Okabayashi *et al.*[7] reported the presence of impurity band states above the extended valence band edge in $Ga_{0.965}Mn_{0.035}As$, as determined by angle-resolved photoemission spectroscopy (ARPES). Additionally, careful optical measurements by Burch *et al.* establish an unusually large hole effective mass ($m^* = 10m_e$), and magnetoresistance measurements by Rokhinson *et al.* suggest the existence of weak localization, both of which indicate that transport occurs within a narrow localized band.[8–10] Finally, magnetic circular dichroism (MCD) measurements provide evidence that ferromagnetism in $Ga_{1-x}Mn_xAs$ is mediated by localized carriers.[11,12] In this paper we present further experimental support for the existence of an impurity band in $Ga_{1-x}Mn_xAs$ and additionally propose a simplified quantitative model for the valence band structure that accurately predicts the optical and electrical behaviors of $Ga_{1-x}Mn_xAs$ and related alloys.

While the MIT concept is valid for semiconductors doped with high concentrations of shallow, nonmagnetic donors and acceptors, which have hydrogenic states of extended nature, its application to magnetic systems is still intensely debated. The localization of holes at Mn atoms is enhanced by disorder (Anderson localization) and *p-d* hybridization. As a result a rather narrow impurity band has been argued to persist at all *x* even though the Mn acceptor level lies only 110 meV above the valence band edge of GaAs.[13] Interestingly, a strong localization of holes at the Mn atoms is suggestive of the behavior found in nonmagnetic Group IV, III–V, and II–VI highly mismatched semiconductor alloys (HMA) such as $GaAs_xN_{1-x}$ and $GaBi_xAs_{1-x}$.[14,15] In these materials, the isoelectronic minority species, As (in $GaAs_xN_{1-x}$) and Bi (in $GaBi_xAs_{1-x}$), have rather low ionization energies compared to those of the element they substitute, inducing a localization of holes at the *p* states of the impurity atoms.

Recent investigations have demonstrated that these localized *p* states undergo an anticrossing interaction with the extended *p* states of the host that causes the valence band of the alloy to restructure into E_+ and E_- subbands. In the case where the localized state is bound within the gap, an impurity band is formed.[14] Thus, the localizing effect of the Mn atoms in $Ga_{1-x}Mn_x$-pnictide materials may lead to an anticrossing-induced reconfiguration of the valence band in DMS systems as well. In fact, the highly localized nature of the transition-metal-associated states in the related DMS $Ga_{1-x}Fe_xN$ has been reported to lead to a renormalization of the valence band of this material.[16] Through an analogous interpretation of the nonmagnetic HMAs, we apply the valence band anticrossing (VBAC) theory to quantitatively detail the formation of a Mn-derived impurity band in $Ga_{1-x}Mn_xAs$.

II. VALENCE BAND ANTICROSSING MODEL

The formation of an impurity band in $Ga_{1-x}Mn_xAs$ is treated theoretically with the VBAC model originally devel-

oped for HMAs. This is a simplified approach that only considers the interaction of host and impurity states of *p*-like symmetry. It is therefore not intended to provide a complete description of the entire valence band structure but does present a valid representation of the impurity band and the valence band edges. The anticrossing interaction between the Mn and GaAs states is treated on the basis of the $\mathbf{k} \cdot \mathbf{p}$ formalism, in which the standard 6×6 Kohn-Luttinger matrix expressing the valence band structure of GaAs is augmented with the six time-reversal symmetry-invariant wave functions of the localized Mn *p* states. A comprehensive description of the model can be found in a previous report.[15] The strength of the interaction and thus the dispersion of the impurity band are primarily influenced by the position of the Mn acceptor level, E_{Mn}, and an empirically determined coupling parameter, C_{Mn}. The coupling parameter provides a numerical assessment of the localization and, in the case of a magnetic species such as Mn, it also includes the complex effects of *p-d* exchange.

One interesting consequence of the anticrossing interaction is that it induces an upward movement of the E_+ impurity band edge with increasing *x* as well as an equal but opposite shift in the E_- valence band edge. As the E_- band states are largely of extended character, this shift can be detected optically by photomodulated reflectance (PR) spectroscopy, which measures the transition energies between critical points in the band structure.[17] The energy separating the E_- valence and conduction-band edges was measured in several $Ga_{1-x-y}Mn_xBe_yAs$ films ($0 < x < 0.041$) grown by molecular-beam epitaxy (MBE). The films had relatively constant hole concentrations of about $4-6 \times 10^{20}$ cm^{-3}, which were determined by an electrochemical capacitance-voltage (ECV) method.[18,19] The probe beam for the optical measurements consisted of a 300 W halogen tungsten lamp dispersed through a 0.5 m monochromator while a chopped HeCd laser ($\lambda = 325$ or 442 nm) was used as the photomodulation source. As is shown in Fig. 1(a), a clear increase in the transition energy compared to that of GaAs is observed only with increasing *x*, indicating a downward shift in the valence band edge. This shift in the band gap is in good agreement with that found in the MCD measurements reported by Beschoten *et al.*[20] and is consistent with the picture of an anticrossing-induced formation of a Mn impurity band. In fact, this same characteristic change in the band-gap energy with alloy composition has been observed in HMAs containing impurity-related bands.[14,21] The experimentally determined trend in the band gap was fit with the VBAC model using a coupling parameter of $C_{Mn} = 0.39$ eV, as shown in Fig. 1(b), under the assumption that the shift predominantly occurs in the valence band. The data points of Beschoten *et al.*, taken at 5 K, were shifted down by 0.1 eV to place them in the context of our room-temperature measurements.[22] The calculated impurity and valence band-edge energies as a function of Mn concentration are shown in Fig. 1(c) as an illustration of the anticrossing behavior.

III. MOBILITY AND METAL-TO-INSULATOR TRANSITION

The impurity band picture offered by the VBAC approach is also able to provide some insight into the transport prop-
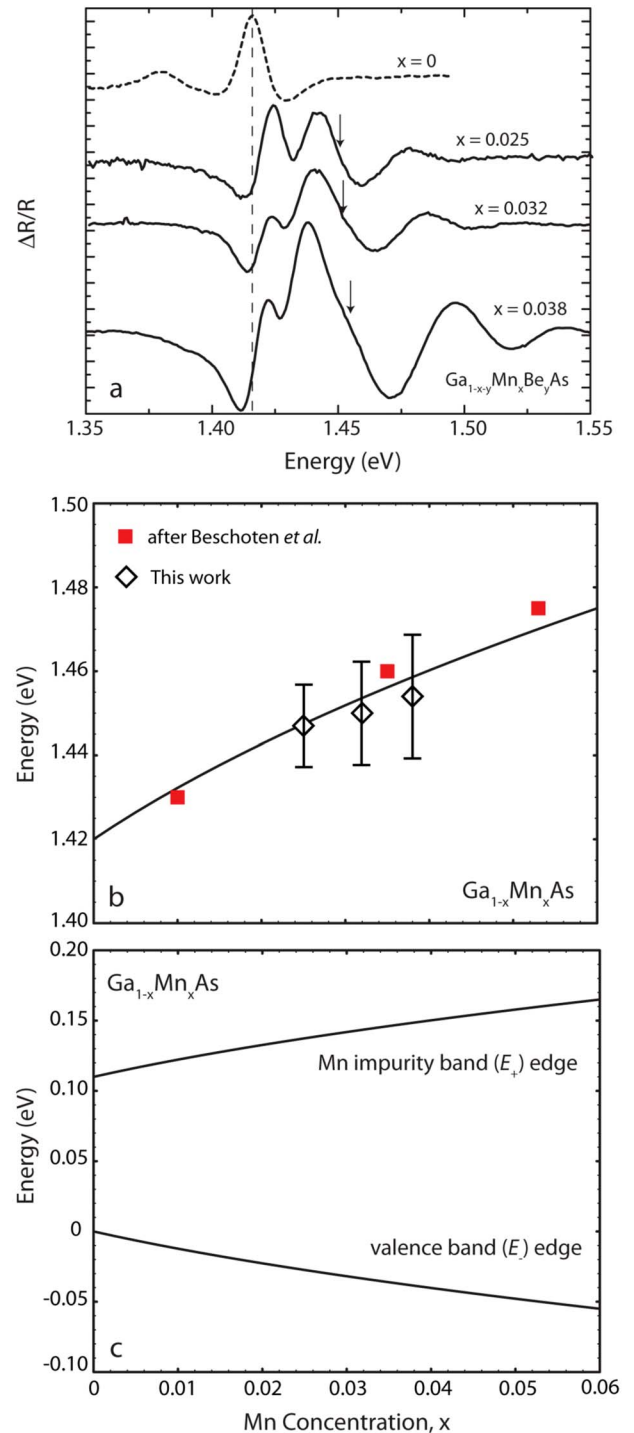

FIG. 1. (a) (Color online) PR spectra of $Ga_{1-x-y}Mn_xBe_yAs$ demonstrate that the valence to conduction-band transition increases in energy with increasing Mn concentration but shows no movement with Be concentration, suggesting an anticrossing interaction between the GaAs and Mn states. The dashed line marks the PR transition of the underlying GaAs substrate while the arrows indicate the transitions of the film. (b) Experimentally determined movement of the band-gap energy of $Ga_{1-x}Mn_xAs$ as well as the theoretical trend predicted by the VBAC model (E_- valence band edge to conduction band) (Ref. 20). (c) Movement of the valence and impurity band-edge energies of $Ga_{1-x}Mn_xAs$ as a function of Mn concentration.
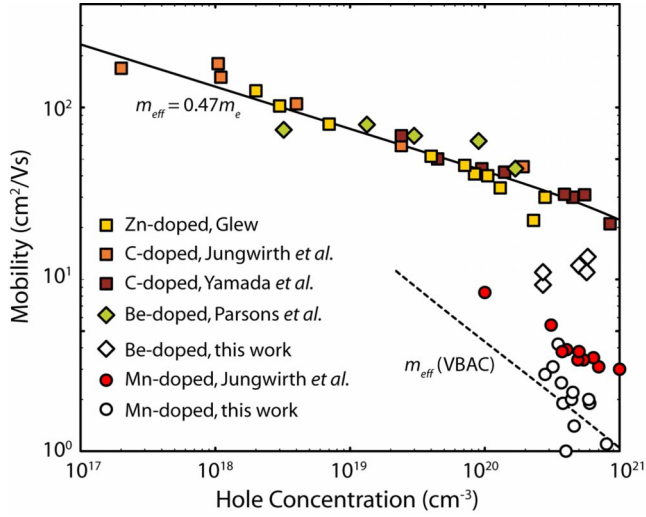
FIG. 2. (Color online) Hole mobility in $Ga_{1-x}Mn_xAs$ and $Ga_{1-x}X_xAs$ (X=Be,C,Zn) as a function of hole concentration (Refs. 23–26). The experimental data of the GaAs samples doped with nonmagnetic acceptors was theoretically fit with an ionized impurity scattering model, using heavy-hole effective masses of m^* =$0.47m_e$. Likewise, the $Ga_{1-x}Mn_xAs$ hole mobility was fit with an effective mass determined by the VBAC model ($\sim m^*$=$30m_e$).

erties of $Ga_{1-x}Mn_xAs$. At the outset of this analysis, though, it is important to note that the transport properties of DMS materials are quite complex and have been shown to be strongly dependent on the concentrations of substitutional and interstitial Mn, as well as the carrier and defect concentrations.[5] Understandably, there will be some variation in experimental measurements based on sample processing and quality. The theoretical calculations presented here are therefore intended to capture only the overall trends and effects of an average and reasonable subset of defect concentrations and compensation ratios.

In DMS alloys the presence of the anomalous Hall effect does not allow for simple measurement of carrier mobilities using this technique. However, as has been shown by Yu and co-workers,[18,19] a combination of ECV and resistivity measurements can be used to accurately determine the mobility. To elucidate the difference in hole transport properties between $Ga_{1-x}Mn_xAs$ and GaAs doped with nonmagnetic hydrogenic acceptors, we have measured hole mobilities in series of GaAs samples doped with either Mn or Be. Both sets of samples were grown under similar conditions. The results, displayed in Fig. 2 along with those reported in the literature, demonstrate that the room-temperature hole mobilities of $Ga_{1-x}Mn_xAs$ ($\mu \sim 1$–5 cm^2/Vs) are consistently about one order of magnitude lower than those observed in GaAs doped with similar concentrations of nonmagnetic acceptors ($\mu \sim 10$–50 cm^2/Vs).[23–26] Furthermore, the experimental data reveal two distinct trends between the magnetic and nonmagnetic samples. This large difference in hole mobilities cannot be explained by spin-disorder scattering, which is proportional to magnetic susceptibility, and therefore it should depend strongly on temperature. In metallic $Ga_{1-x}Mn_xAs$, zero-field resistivity is very weakly dependent on the temperature, suggesting that spin disorder cannot be

the dominant mechanism limiting the mobility.

Therefore, ionized impurity scattering is considered to be the dominant mobility limiting mechanism in both the $Ga_{1-x}X_xAs$ (X=Be,C,Zn) and $Ga_{1-x}Mn_xAs$ samples examined here. Since the two sets of samples were grown under similar conditions, the consistently large disparity in the hole mobility values may be attributed primarily to a difference of the hole effective masses in the two cases. The hole mobility was calculated using a standard expression for the ionized impurity scattering:[27]

$$\mu_{II} = \frac{\varepsilon^2 k_F}{2\pi e^3 \hbar N_i \left[\ln(1+\xi) - \dfrac{\xi}{1+\xi} \right]} \left(\frac{dE}{dk} \right)^2, \quad (1)$$

where ε is the dielectric constant, k_F is the Fermi wave vector, N_i is the concentration of ionized impurities, and

$$\xi = (2k_F R)^2. \quad (2)$$

Here R is the screening length for a degenerate gas, given as

$$\frac{1}{R^2} = \left(\frac{3p}{\pi} \right)^{1/3} \frac{4m_{\text{eff}} e^2}{\varepsilon \hbar^2}, \quad (3)$$

where p is the carrier concentration and the heavy-hole effective mass, m_{eff}, is taken at the Fermi level.[27]

The experimental hole mobility in $Ga_{1-x}X_xAs$ (X =Be,C,Zn) can be explained theoretically when assuming the standard heavy-hole effective mass of GaAs (m_{eff} =$0.47m_e$) by adopting an average ionized impurity center concentration of N_i=$2.5p$. Although large, this impurity concentration is still plausible when one considers the difficulty of doping GaAs p type with such large hole concentrations since defects tend to be quite prevalent in GaAs-based thin films grown at the low temperatures necessary to incorporate dopants at high levels. Thus, the significant scatter in the mobility at high doping concentrations is due in part to differences in the film growth temperature. In contrast, using the same effective mass to account for the low hole mobility values in $Ga_{1-x}Mn_xAs$ requires an unrealistically large ionized impurity concentration of N_i=3×10^{22} cm^{-3} for films with hole concentrations of p=8×10^{20} cm^{-3}. Instead, a more reasonable justification for the greatly reduced hole mobility may be realized by considering an increase in m_{eff}, where calculations show that the trend in our experimental data may be fit with the same ionized impurity concentration N_i=$2.5p$ and a large VBAC-derived hole effective mass upward of $30m_e$.

Such a large hole effective mass is consistent with the impurity band perspective and can readily be accounted for by the VBAC model. Figure 3 displays the theoretical hole dispersion relations of the Mn-derived bands in $Ga_{0.99}Mn_{0.01}As$ and $Ga_{0.96}Mn_{0.04}As$, which were calculated with the model parameters outlined in the preceding section. The composition dependence of the corresponding hole masses may be determined from the derivative of the dispersion relation and the Fermi wave vector, k_F, through the following relationship:
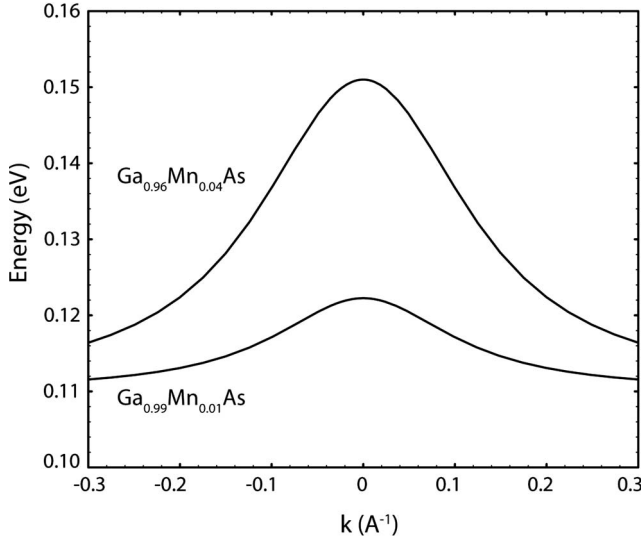
FIG. 3. Dispersions of the impurity band in $Ga_{0.99}Mn_{0.01}As$ and $Ga_{0.96}Mn_{0.04}As$, illustrating the increase in the width of the impurity band with increasing Mn concentration.

$$m_{\text{eff}} = \frac{\hbar k}{\partial E/\partial k} \quad \text{at} \quad k = k_F. \tag{4}$$

As is shown in Fig. 4, the VBAC model predicts a very large heavy-hole mass in samples with low Mn concentrations assuming 40% compensation, which is reasonable for many as-grown $Ga_{1-x}Mn_xAs$ films. The magnitude of m_{eff} is a reflection of the very narrow and flat nature of the Mn-derived band and is also in agreement with the well-established observation of nonmetallic conduction in $Ga_{1-x}Mn_xAs$ with small x.[28–30] Upon further addition of Mn, the impurity bandwidth increases, causing a reduction in the hole effective mass until it reaches a value of $m_{\text{eff}} = 33-35m_e$ for $x > 0.015$. Although uncommonly large, these theoretically determined values are of the same magnitude as those reported by Burch *et al.*[8] The corresponding $Ga_{1-x}Mn_xAs$ hole mobilities, calculated by Eq. (1) assuming

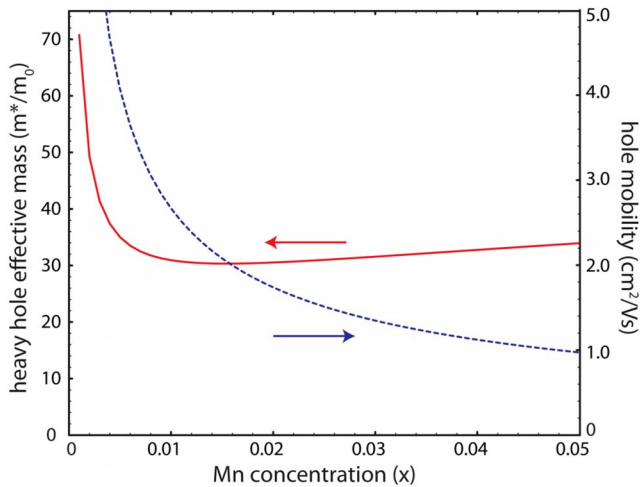FIG. 4. (Color online) $Ga_{1-x}Mn_xAs$ heavy-hole effective mass and mobility as a function of Mn concentration.
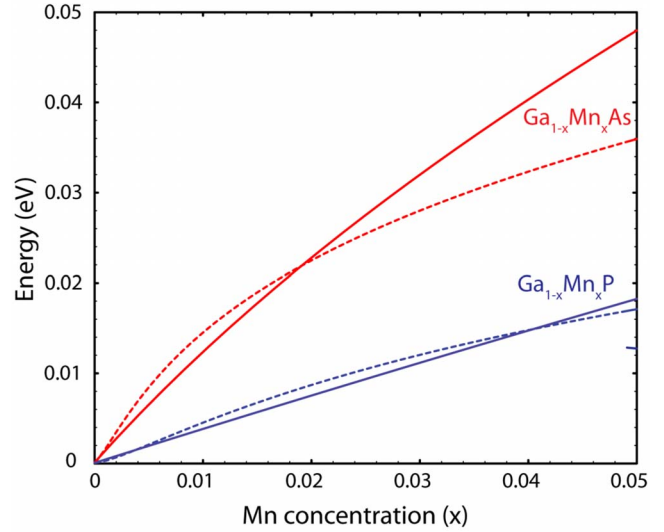

FIG. 5. (Color online) Impurity bandwidth (solid lines) and heavy-hole lifetime broadening (dashed lines) for $Ga_{1-x}Mn_xAs$ and $Ga_{1-x}Mn_xP$ as a function of Mn concentration.

40% compensation and $N_i = 1.4p$, are also displayed in Fig. 4. These theoretical mobility values fall within the range of those measured experimentally, as shown in Fig. 2 for a comparable set of Mn concentrations and compensation ratios. We note that the tenfold reduction in the mobility that results from an approximately 60-fold increase in m_{eff} is a reflection of the relatively weak dependence of the mobility on the effective mass for long-range coulomb scattering potentials.

The quantitative analysis of the $Ga_{1-x}Mn_xAs$ valence band structure provided by the VBAC model also offers an explanation of how a MIT may occur within the impurity band. On the basis of the Zener model, the MIT in $Ga_{1-x}Mn_xAs$, found to occur at roughly $x = 0.02$, is thought to transpire when the hopping conduction in the impurity band gives way to transport in the valence band after the two merge. However, a MIT can occur within an impurity band if the scattering of carriers within the band is altered such that extended transport becomes possible. This transition may be assessed in terms of the lifetime broadening of the hole energies, determined from their mass and mobility through the relationship,

$$\delta E = \frac{\hbar e}{\mu m_{\text{eff}}}. \tag{5}$$

If the energy uncertainty is greater than the width of the impurity band, as is typically the case in minimally Mn-doped $Ga_{1-x}Mn_xAs$ ($x < 0.02$), then transport is dominated by the hopping mechanism, rendering the material an insulator. With an increase in the Mn concentration, though, the localized states comprising the impurity band take on a more extended character through hybridization with the valence band, and the band widens. The MIT then occurs when the impurity bandwidth exceeds the lifetime broadening, as is illustrated in Fig. 5 for $Ga_{1-x}Mn_xAs$, considering the previously assumed compensation ratio and ionized impurity center concentration. Obviously, the MIT will shift to a larger x

upon a decrease in the crystal quality, which is typically observed in experimental investigations.

IV. METAL TO INSULATOR TRANSITIONS IN $Ga_{1-x}Mn_xAs_{1-y}V_y$ ALLOYS

The concept of the anticrossing-induced formation of a Mn-derived impurity band is not unique to $Ga_{1-x}Mn_xAs$ but may also be used to explain the transport properties of other $Ga_{1-x}Mn_x$-pnictide compounds and their alloys. For example, it has been demonstrated that an impurity band does exist in $Ga_{1-x}Mn_xP$ up to high Mn concentrations ($x > 0.04$).[24] From the VBAC perspective, the strength of the anticrossing interaction in this system is reduced due to the rather large separation of the Mn acceptor level from the GaP valence band edge ($E_{Mn} = 0.4$ eV), causing the impurity band to remain localized in nature. Theoretical analysis of the lifetime broadening in $Ga_{1-x}Mn_xP$, performed within the scheme of the VBAC model, demonstrates that the MIT is shifted to higher Mn concentrations of approximately $x > 0.04$, as shown in Fig. 5. Because the exact value of the coupling parameter was not determined from optical measurements, as in the case of $Ga_{1-x}Mn_xAs$, a value of $C_{Mn} = 0.39$ eV was also applied to these calculations. However, chemical trends suggest that the *p-d* exchange-related coupling parameter should increase slightly as the anion species changes from As to P. Taking this alteration into consideration, the MIT in $Ga_{1-x}Mn_xP$ would extend to a moderately higher Mn concentration in agreement with experimental observations that indicate the persistence of hopping conduction for all samples in the concentration range $0 < x < 0.042$.[31]

The large effective mass of the holes in the Mn-derived band has important consequences for the transport properties of Mn-doped ternary alloys. A recent experimental investigation into the transport behavior of $Ga_{1-x}Mn_xAs_{1-y}P_y$ demonstrated that the addition of just a few percent of P ($y \sim 0.016-0.024$) to $Ga_{0.954}Mn_{0.046}As$ converts the transport behavior of the alloy from metallic to insulating.[32] Likewise, an even greater transformation of the transport properties occurs in $Ga_{0.954}Mn_{0.046}As_{1-y}N_y$ alloys where the MIT is found to arise at an extremely low N concentration of roughly $y = 0.003-0.004$.[32–35] Such unexpected behavior cannot be adequately explained by the slight change in the valence band structure or the Mn acceptor binding energy upon the addition of very dilute concentrations of P or N. However, a change in alloy disorder scattering, which is strongly mass dependent, will significantly affect the mobility of the very heavy holes in the impurity band. The mobility limited by alloy disorder scattering is given by[36]

$$\mu_{AD} = \frac{h^3 e}{8\pi^2 m_{eff}^2 k_F |V_{AD}|^2 \Omega y},\qquad(6)$$

where Ω is the unit-cell volume, and the scattering potential, V_{AD}, is assumed to be the offset of the impurity band edges in $Ga_{1-x}Mn_xAs$ and $Ga_{1-x}Mn_xP$. In the context of the Zener model, the Mn states have merged with the GaAs valence band at this concentration of $x = 0.046$ substitutional Mn atoms and the addition of P or N should only shift the valence band edge downward in energy slightly (~ 4 or 20 meV per
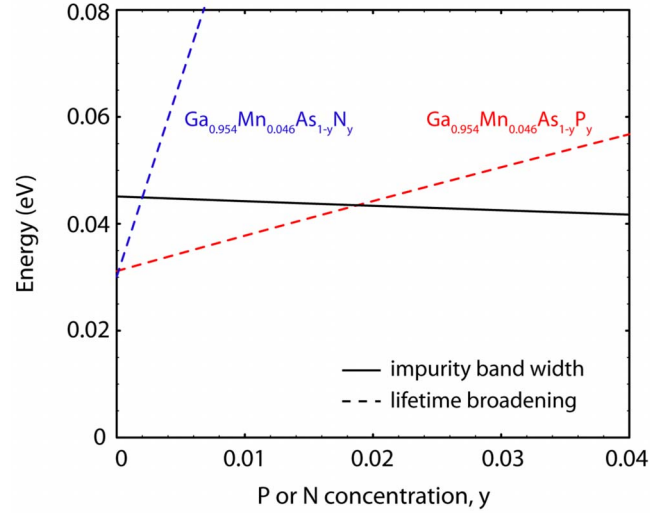

FIG. 6. (Color online) Impurity bandwidth (solid line) and heavy-hole lifetime broadening (dashed line) for $Ga_{1-x}Mn_xAs_{1-y}P_y$ ($Ga_{1-x}Mn_xAs_{1-y}N_y$) as a function of P (N) concentration, y (Ref. 32).

$y = 0.01$ for P and N, respectively). Under the assumption of a relatively low heavy-hole effective mass at the Fermi level on the order of that found in GaAs, the sheet resistance of a 30 nm $Ga_{0.954}Mn_{0.046}As_{1-y}P_y$ or $Ga_{0.954}Mn_{0.046}As_{1-y}N_y$ film should shift approximately only $10-100$ $\Omega/\square$ upon the addition of $y = 0.01$.

The VBAC approach, which is predicated on the dependence of the carrier transport on the alloying-induced energy uncertainty, provides a more plausible explanation of the large drop in conductivity in Mn-doped ternary alloys. Substitution of the VBAC-determined impurity band hole effective masses into Eq. (4) allows for the calculation of the alloy disorder scattering-limited mobility and the broadening parameter. Our theoretical predictions, shown in Fig. 6, clearly substantiate the experimentally observed MIT in both alloys.[32] In the case of $Ga_{0.9594}Mn_{0.046}As_{1-y}P_y$, the energy uncertainty is found to increase quite considerably, surpassing the impurity bandwidth at approximately $y = 0.018$ for a fixed Mn concentration of $x = 0.046$ and a $V_{AD} = 0.21$ eV. Likewise, the MIT in $Ga_{0.959}Mn_{0.041}As_{1-y}N_y$ occurs when the energy uncertainty exceeds the impurity bandwidth and is shifted to even lower y values due to the enhanced scattering potential. While the exact value of V_{AD} in $Ga_{0.959}Mn_{0.041}As_{1-y}N_y$ cannot be established as the valence band offset between GaAs and zinc-blende (ZB) GaN is not explicitly known, comparison of ZB and wurtzite (WZ) GaN combined with an assumed Mn acceptor level located 1.4 eV above the valence band edge of WZ GaN suggests that $V_{AD} = 0.5-0.7$ eV. Calculations of the alloy disorder scattering with $V_{AD} = 0.7$ eV estimate that the MIT occurs around $y = 0.002$, in reasonable agreement with the experimental findings.

Although the VBAC model does not explicitly treat the fundamental origin of ferromagnetism in these materials, its description of their transport properties can be used to qualitatively corroborate the general experimentally observed trends in T_c as a function of alloy composition. In the scheme

of the Ruderman-Kittel-Kasuya-Yosida (RKKY)-Zener model, theoretical calculations have demonstrated that the T_c decreases as the mean-free path of the carriers is reduced.[37] The hole mean-free path may be calculated as

$$l = \upsilon_F \tau = \frac{h k_F \mu}{e}. \qquad (7)$$

Using this line of argument, it is clear from the VBAC calculations that the T_c of $Ga_{1-x}Mn_xP$ should be lower than that of $Ga_{1-x}Mn_xAs$ due to its diminished mobility. Likewise, the sharp drop in the T_c observed in $Ga_{0.959}Mn_{0.041}As_{1-y}P_y$ with increasing y is also consistent with this picture as the presence of P greatly affects the carrier relaxation time.[32] Physically, this relationship can be understood by considering that the number of Mn spins coupled by an itinerant hole is reduced as the distance the hole travels between scattering events decreases. It must be stressed here that, although limited in scope, the analysis indicates that the Mn-impurity band description is congruous with the current view of ferromagnetic behavior of these materials.

V. CONCLUSION

In summary, many of the optical and transport properties of $Ga_{1-x}Mn_xAs$ previously unexplained by the Zener model may be understood from the perspective of a sustained Mn-derived impurity band described by the VBAC model. The formation of the impurity band arises as the result of an anticrossing interaction between the localized and extended p states of the Mn atoms and GaAs host, respectively, which increases in strength with Mn concentration. Most importantly, the VBAC model provides a quantitative assessment of the impurity band, including the bandwidth and carrier mass, which is capable of addressing the unusually low mobilities, as well as the MIT in $Ga_{1-x}Mn_x$-V compounds and their alloys.

*Corresponding author; W_Walukiewicz@lbl.gov

[1] T. Dietl, H. Ohno, F. Matsukura, J. Cibert, and D. Ferrand, Science **287**, 1019 (2000).

[2] A. H. MacDonald, P. Schiffer, and N. Samarth, Nat. Mater. **4**, 195 (2005).

[3] N. F. Mott, Rev. Mod. Phys. **40**, 677 (1968).

[4] Y. Zhang and S. Das Sarma, Phys. Rev. B **72**, 125303 (2005).

[5] E. H. Hwang and S. Das Sarma, Phys. Rev. B **72**, 035210 (2005).

[6] S. Sanvito, P. Ordejon, and N. A. Hill, Phys. Rev. B **63**, 165206 (2001).

[7] J. Okabayashi, A. Kimura, O. Rader, T. Mizokawa, A. Fujimori, T. Hayashi, and M. Tanaka, Phys. Rev. B **64**, 125304 (2001).

[8] K. S. Burch, D. B. Shrekenhamer, E. J. Singley, J. Stephens, B. L. Sheu, R. K. Kawakami, P. Schiffer, N. Samarth, D. D. Awschalom, and D. N. Basov, Phys. Rev. Lett. **97**, 087208 (2006).

[9] L. P. Rokhinson, Y. Lyanda-Geller, Z. Ge, S. Shen, X. Liu, M. Dobrowolska, and J. K. Furdyna, Phys. Rev. B **76**, 161201(R) (2007).

[10] D. Neumaier, K. Wagner, S. Geiszler, U. Wurstbauer, J. Sadowski, W. Wegscheider, and D. Weiss, Phys. Rev. Lett. **99**, 116803 (2007).

[11] R. Chakarvorty, S. Shen, K. J. Yee, T. Wojtowicz, R. Jakiela, A. Barcz, X. Liu, J. K. Furdyna, and M. Dobrowolska, Appl. Phys. Lett. **91**, 171118 (2007).

[12] K. Ando, H. Saito, K. C. Agarwal, M. C. Debnath, and V. Zayets, Phys. Rev. Lett. **100**, 067204 (2008).

[13] K. S. Burch, D. D. Awschalom, and D. N. Basov (unpublished).

[14] J. Wu, W. Walukiewicz, K. M. Yu, J. D. Denlinger, W. Shan, J. W. Ager, A. Kimura, H. F. Tang, and T. F. Kuech, Phys. Rev. B **70**, 115214 (2004).

[15] K. Alberi, J. Wu, W. Walukiewicz, K. M. Yu, O. D. Dubon, S. P. Watkins, C. X. Wang, X. Liu, Y.-J. Cho, and J. Furdyna, Phys. Rev. B **75**, 045203 (2007).

[16] W. Pacuski, P. Kossacki, D. Ferrand, A. Golnik, J. Cibert, M. Wegscheider, A. Navarro-Quezada, A. Bonanni, M. Kiecana, M. Sawicki, and T. Dietl, Phys. Rev. Lett. **100**, 037204 (2008).

[17] D. E. Aspnes, Surf. Sci. **37**, 418 (1973).

[18] K. M. Yu, W. Walukiewicz, T. Wojtowicz, W. L. Lim, X. Liu, U. Bindley, M. Dobrowolska, and J. K. Furdyna, Phys. Rev. B **68**, 041308(R) (2003).

[19] K. M. Yu, W. Walukiewicz, T. Wojtowicz, W. L. Lim, X. Liu, Y. Sasaki, M. Dobrowolska, and J. K. Furdyna, Appl. Phys. Lett. **81**, 844 (2002).

[20] B. Beschoten, P. A. Crowell, I. Malajovich, D. D. Awschalom, F. Matsukura, A. Shen, and H. Ohno, Phys. Rev. Lett. **83**, 3073 (1999).

[21] K. M. Yu, W. Walukiewicz, J. Wu, W. Shan, J. W. Beeman, M. A. Scarpulla, O. D. Dubon, and P. Becla, Phys. Rev. Lett. **91**, 246403 (2003).

[22] L. G. Shantharama, A. R. Adams, C. N. Ahmad, and R. J. Nicholas, J. Phys. C **17**, 4429 (1984).

[23] R. W. Glew, J. Cryst. Growth **68**, 44 (1984).

[24] T. Jungwirth, J. Sinova, A. H. MacDonald, B. L. Gallagher, V. Novak, K. W. Edmonds, A. W. Rushforth, R. P. Campion, C. T. Foxon, L. Eaves, E. Olejnik, J. Masek, S. R. Eric Yang, J. Wunderlich, C. Gould, L. W. Molenkamp, T. Dietl, and H. Ohno, Phys. Rev. B **76**, 125206 (2007).

[25] T. Yamada, E. Tokumitsu, K. Saito, T. Akatsuka, M. Miyauchi, M. Konagai, and K. Takahashi, J. Cryst. Growth **95**, 145 (1989).

[26] J. D. Parsons and F. G. Krajenbrink, J. Electrochem. Soc. **130**, 1782 (1983).

[27] W. Zawadzki and W. Szymanska, Phys. Status Solidi B **45**, 415 (1971).

[28] W. Allen, E. G. Gwinn, T. C. Kreutz, and A. C. Gossard, Phys. Rev. B **70**, 125320 (2004).

[29] S. Shen, X. Liu, Z. Ge, J. K. Furdyna, M. Dobrowolska, and J. Jaroszynski, J. Appl. Phys. **103**, 07D134 (2008).

[30] B. L. Sheu, R. C. Myers, J.-M. Tang, N. Samarth, D. D. Awschalom, P. Schiffer, and M. E. Flatte, Phys. Rev. Lett. **99**, 227205 (2007).

[31] M. A. Scarpulla, B. L. Cardozo, R. Farshchi, W. M. Hlaing Oo, M. D. McCluskey, K. M. Yu, and O. D. Dubon, Phys. Rev. Lett. **95**, 207204 (2005).

[32] P. R. Stone, K. Alberi, S. K. Z. Tardif, J. W. Beeman, K. M. Yu, W. Walukiewicz, and O. D. Dubon, Phys. Rev. Lett. (to be published).

[33] R. Kling, A. Koder, W. Schoch, S. Frank, M. Oettinger, W. Limmer, R. Sauer, and A. Waag, Solid State Commun. **124**, 207 (2002).

[34] G. Kobayashi, T. Mori, T. Kato, T. Hanada, H. Makino, and T. Yao, J. Cryst. Growth **301-302**, 642 (2007).

[35] I. Oshiyama, T. Kondo, and H. Munekata, J. Appl. Phys. **98**, 093906 (2005).

[36] J. W. Harrison and J. R. Hauser, Phys. Rev. B **13**, 5347 (1976).

[37] S. Das Sarma, E. H. Hwang, and D. J. Priour, Jr., Phys. Rev. B **70**, 161203(R) (2004).